Eur Biophys J (1998) 27: 431–436

ARTICLE

Kenneth H. Downing · Eva Nogales

New insights into microtubule structure and function from the atomic model of tubulin

Received: 15 December 1997 / Revised version: 25 January 1998 / Accepted: 2 February 1998

Abstract The structure of tubulin has recently been solved by electron crystallography of zinc-induced tubulin sheets. Because tubulin was studied in a polymerized state, the model contains information on the interactions between monomers that give rise to the $\alpha\beta$ dimer as well as contacts between adjacent dimers that result in the structure of the protofilament. The model includes the binding site of taxol, an anti-cancer agent that acts by stabilizing microtubules. The present tubulin model gives the first structural framework for understanding microtubule polymerization and its regulation by nucleotides and anti-mitotic drugs at the molecular level.

Key words Tubulin · Microtubules · Electron crystallography · Taxol · Colchicine

Introduction

The many roles served by microtubules make them essential to the life of all eukaryotic cells. These critical functions along with their fascinating biophysical properties have made microtubules interesting to scientists from many disciplines who have sought to understand the mechanisms that are involved in microtubule functions in the cell. The wealth of data that has been gathered over the years has led to many significant insights, but the interpretation of the data has been incomplete without knowledge of the basic structure of tubulin, the main protein component of microtubules. The tendency of tubulin to polymerize, which is an essential property for microtubule formation, results in a number of polymeric forms besides microtubules. Among these are 2-dimensional crystalline sheets, first described over thirty years ago (Larsson et al. 1976), that form in the presence of Zn^{++} and are thus frequently referred to as "zinc-sheets." This polymer is well suited to study by electron crystallography, a technique that has recently developed as a complement to x-ray crystallography in studies of small, especially thin, crystals. Earlier we had shown that these crystals could provide high-resolution structural information (Downing and Jontes 1992; Nogales et al. 1995), and we have now extended the previous work with the determination of an atomic model of the tubulin dimer from electron crystallographic data at 3.7 Å resolution (Nogales et al. 1998a).

K. H. Downing (✉) · E. Nogales
Life Science Division,
Lawrence Berkeley National Laboratory,
Berkeley, CA 94720, USA
e-mail: KHDowning@lbl.gov

Tubulin structure

Figure 1 shows ribbon diagrams of the tubulin structure in views corresponding to the inside and outside of the microtubule. The structures of α and β tubulin are very similar, with identical topology and differences mainly limited to loop regions. Each monomer is formed by a pair of central beta sheets surrounded by helices. The relation between the sequence and structure is shown in Fig. 2. The α and β tubulin sequences are aligned, and residue numbering is based on that alignment and includes two gaps in the sequence of β tubulin. We previously identified which subunit is β (Nogales et al. 1995) based on the preferential binding of taxol (Rao et al. 1994). Determination of the inside-outside orientation of the protofilament as it would be in a microtubule was based on correlation of the lower resolution maps with freeze-fracture images and 3-D reconstructions of microtubules (Wolf et al. 1996). Most of the outside surface of the microtubule is formed by a pair of antiparallel helices with a long connecting loop. The helices appear to form most of the surface that interacts with motor molecules, while the loop is involved in contacts between monomers along the protofilaments. The last 10 residues at the C-terminus of α, and 18 in β, are not resolved in the map, presumably due to disorder resulting from their high charge density, but they are clearly located on the outside of the microtubule. Previous evidence had

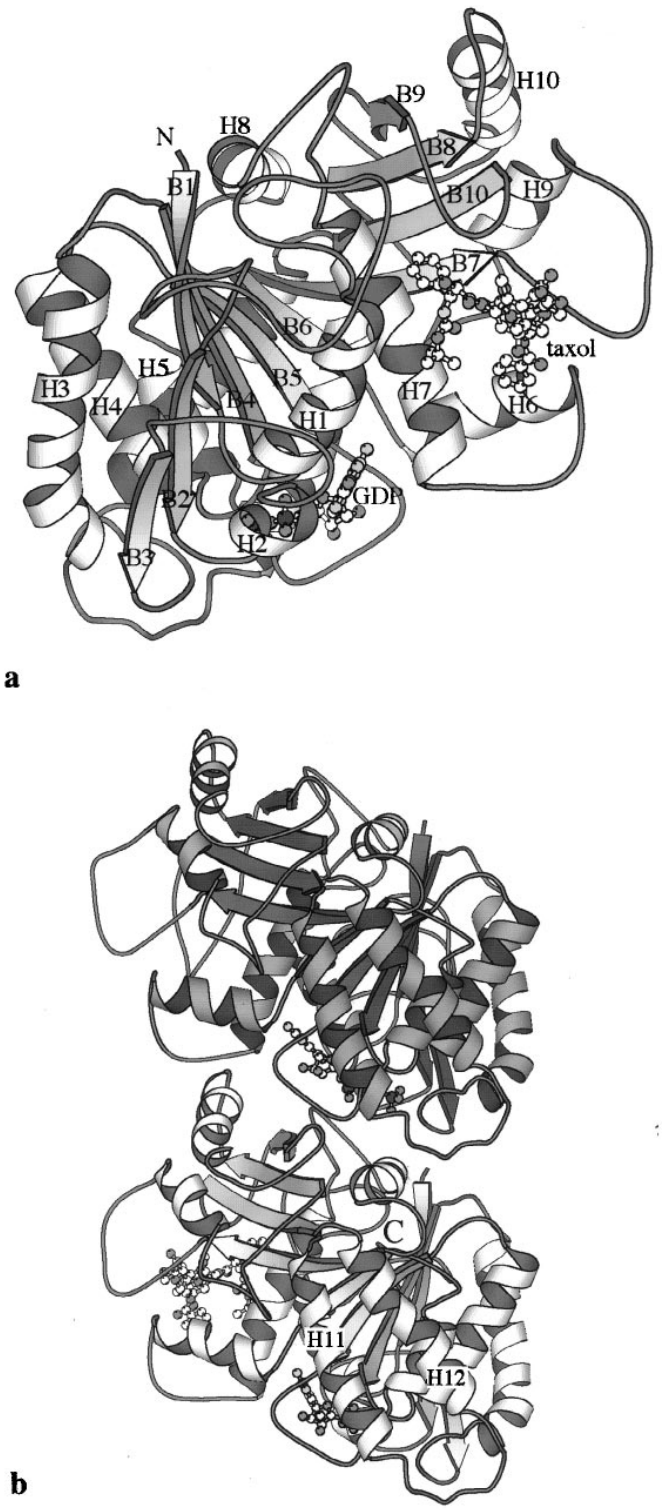

Fig. 1 **a** Ribbon diagram of the β monomer viewed from the inside of a microtubule. Helical segments (H1–H10) and beta strands (B1–B10) are marked to allow correlation with the sequence (see Fig. 2). **b** View of the dimer from the outside of a microtubule. The β monomer, on the bottom, is shown in a lighter gray. Helices H11 and H12 are marked in this view, which also shows the longitudinal interaction between monomers. The plus end of the microtubule is down in this figure (see text)

also indicated that the C-terminus must be accessible for interaction with MAPs on the outside of the microtubule (Cross et al. 1991).

The N-terminal section of the sequence forms a Rossmann fold of alternating alpha helices and parallel beta strands that constitutes the nucleotide binding domain in each monomer. It has previously been recognized that tubulin shares little sequence homology with other GTP-binding proteins, and there was some expectation that the structure would be substantially different. The tubulin topology is different from that of the classical GTPases, with altered connectivity among some of the strands and different nucleotide binding strategy (Nogales et al. 1998b). These differences make if difficult to identify elements in tubulin that would correspond to the switch regions in proteins such as p21 Ras, EF-Tu or transducin. The signature motif of tubulins, a glycine-rich loop of residues GGGTGSG, interacts with the phosphates as predicted by analogy with the P loop of the GTPases (Mandelkow et al. 1985). There are in fact interactions with the nucleotide in each of the loops that link the first six beta strands with the subsequent helices. At the end of the monomer opposite the nucleotide binding site are residues between H7 and H8 that had been predicted to interact with the nucleotide, based on comparisons with GAPDH and other nucleotide-binding proteins (Mandelkow et al. 1985). This region in each of the monomers approaches the nucleotide in the adjacent monomer. The fact that hydrolysis follows polymerization suggests that this part of the structure acts as a GTPase activator, either directly in a way similar that in the Ras-GAP complex (Scheffzek et al. 1997) or indirectly by influencing the conformation of the adjacent monomer around the γ phosphate.

The location of the nucleotide binding site at the surface of the monomer suggests both the polarity of the monomer and the boundary of the dimer. It is known that the nucleotide in β is exchangeable in the dimer, while the nucleotide in α is not exchangeable under normal conditions. Thus it is most reasonable to expect that the dimer is as shown in Fig. 1b, with the nucleotide in α buried at the interface between α and β monomers. Furthermore, it has been shown that the nucleotide in β can exchange with the solution at the plus end, but not at the minus end, of a microtubule (Mitchison 1993). This follows simply from our dimer model if the dimer is oriented with the β subunit at the plus end, so that the nucleotide in β is exposed at the surface of the dimer as well as at the microtubule plus end. Further evidence that β tubulin is at the plus end comes from images of the ends of motor-decorated microtubules opened into sheets (Hirose et al. 1995) and the observation that an anti-α antibody binds only at the minus ends (Fan et al. 1996).

Our previous studies on the comparison of images of negatively-stained sheets and opened microtubule ends (Wolf et al. 1996) had led us to the opposite conclusion, that α tubulin was the subunit crowning the plus end. We have now generated projections of the protofilaments as they would appear in the zinc and microtubule sheets using the tubulin atomic model in order to understand why

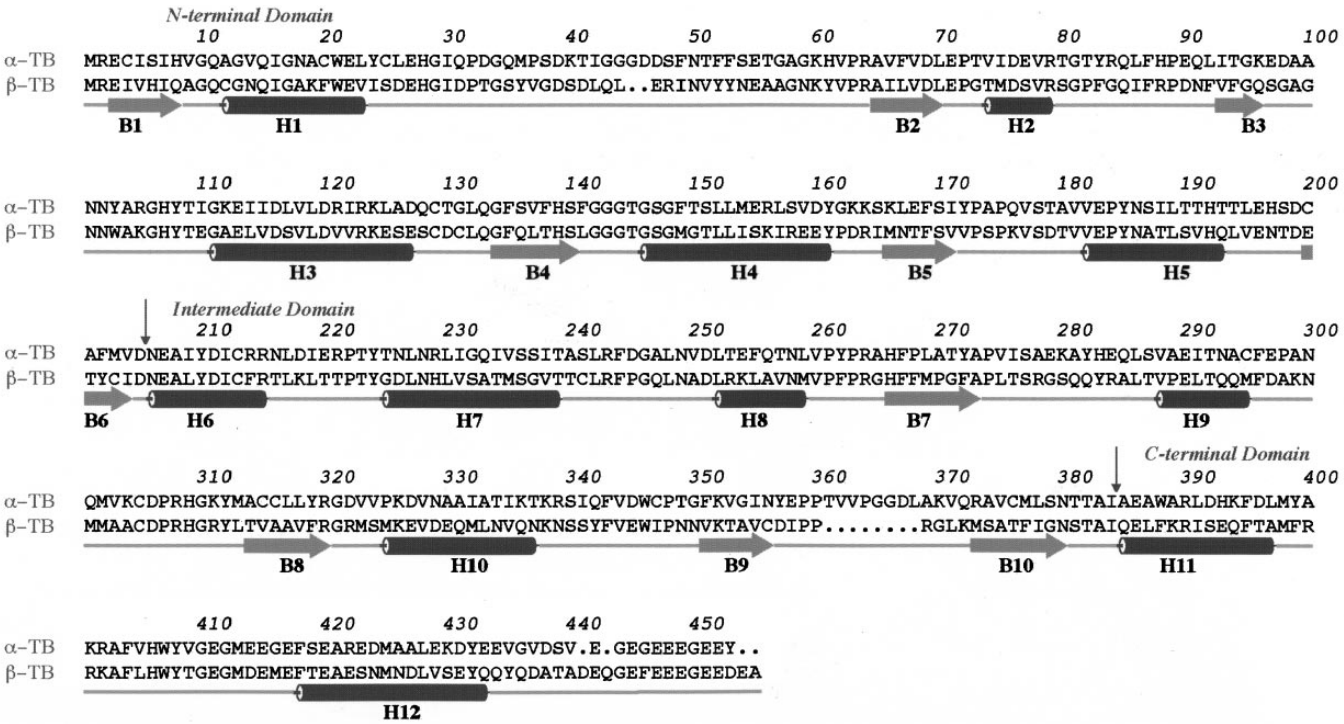

Fig. 2 Sequences of α and β tubulin as used in building the atomic model, and secondary structure assignments. All of the experimental work has been done with bovine brain tubulin, but in the absence of sequences from cow, we have used the pig sequences (Krauss et al. 1981), which are expected to be virtually identical. The numbering used in the text corresponds to that of Kraus et al. (1981) in order to relate most clearly to the structure. Secondary structure elements, corresponding to the labels of Fig. 1, are marked

we previously came to the wrong conclusion. It is now clear that a rotation of about 20 degrees around the protofilament axis is required to fit the protofilament into a microtubule (manuscript in preparation). Figure 3 shows projections of the atomic model calculated with limited resolution and viewed as they are seen in the zinc sheets and as they are presumed to be in microtubules. In the negative stain images there is a continuous band of density that runs along the protofilament near one edge (Wolf et al. 1996). The relative polarities of the two sheets had been interpreted on the basis of the position of this band and on the asymmetry of the monomer projections. As seen in Fig. 3, rotation of the protofilament moves the center of mass and changes the asymmetry in these low resolution images in a way that suggests an inversion of the protofilament direction.

The position of the nucleotide in β at the interface between dimers also suggests the nature of the conformational change that has been proposed to follow hydrolysis of the nucleotide. Given that the nucleotide state is different in the two monomers of the model, the similarity of the structures of α and β, especially around the nucleotide, is remarkable. However, it is now recognized that in microtubules hydrolysis induces some stress in the structure, but the lattice contacts between dimers keep the structure close

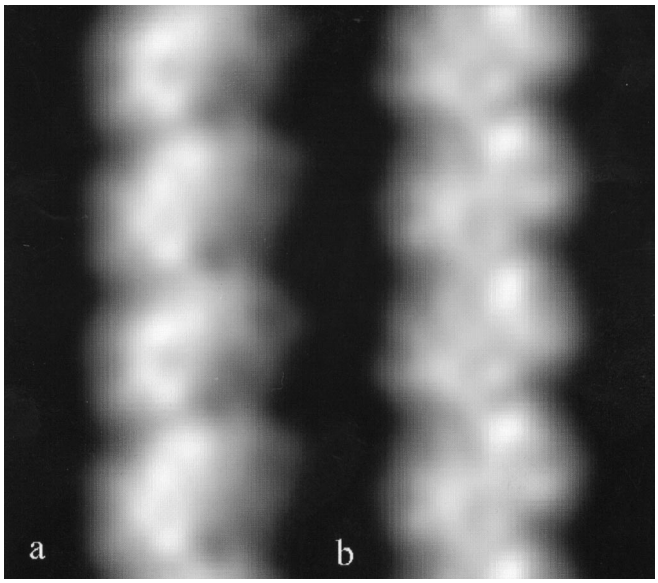

Fig. 3 a, b Projections of the atomic model calculated with low resolution (6 Å resolution cutoff, temperature factor B = 1000) to approximate images of negatively-stained samples. **a** Orientation as seen in the zinc sheets, with plus end down. **b** Rotated 20 degrees around protofilament axis corresponding to orientation in a microtubule, and rotated 180 degrees around axis perpendicular to the plane of the figure, i.e. plus end up

to that of the GTP-bound state (Caplow et al. 1994). Upon rapid disassembly of microtubules, the protofilaments peel off and curl. In addition, tubulin-GDP can be made to polymerize into closed rings and double rings of about 14–16 dimers. Thus the tubulin-GDP state has become known as the curved conformation, and the tubulin-GTP state as the

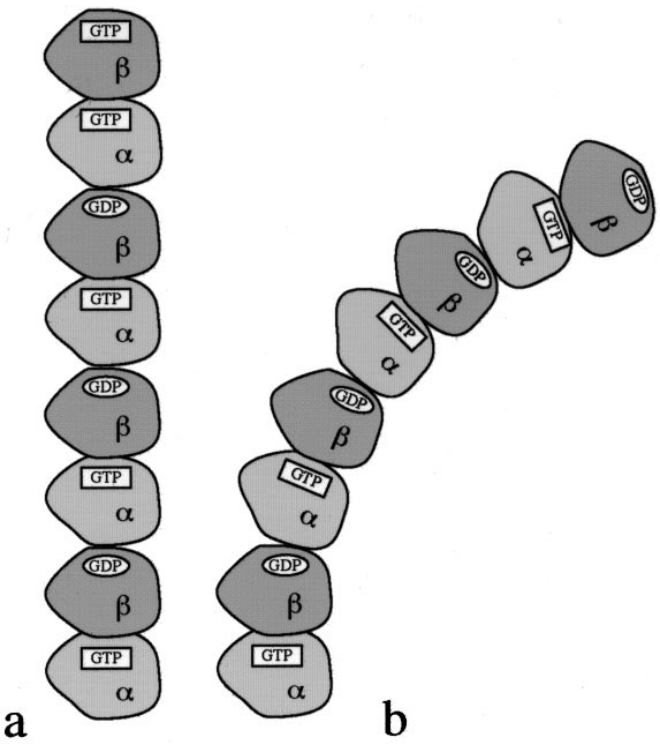

Fig. 4a, b Protofilament models. **a** A protofilament containing GTP in all the exchangeable sites of β is straight, as is a protofilament in a microtubule even after GTP is hydrolyzed to GDP. As GDP-containing protofilaments disassemble from a microtubule, they curl, possibly by kinking at the inter-dimer interface near the exchangeable nucleotide site

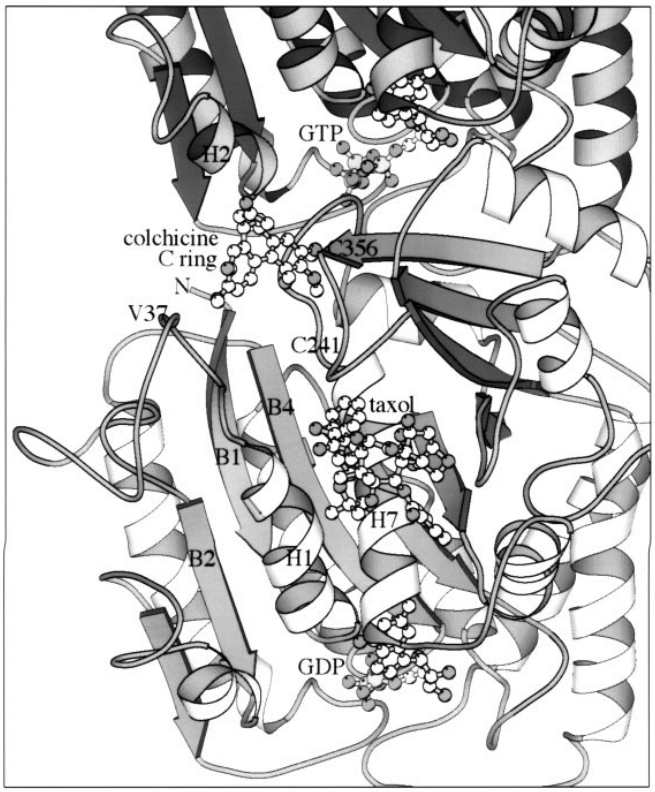

Fig. 5 Hypothetical model of colchicine-tubulin interaction. The orientation corresponds to the view from the left side of Fig. 1b, with the inside of the microtubule on the left of this figure. A model of colchicine has been positioned in a way that agrees with available data on the binding site. The C ring sits between Cys356 and the loop containing Cys241 in β, the A ring is adjacent to the loop near the N terminus containing Val37, and the B ring faces the α monomer. Both colchicine and taxol bind on the side of tubulin that faces the lumen of the microtubule, with colchicine near the α-β interface and taxol bound within the β monomer

straight conformation. We have proposed that the curving seen in the GDP state may reflect a conformational change that occurs mainly at the dimer interface producing a kink between dimers, as illustrated in Fig. 4 (Downing and Nogales 1998).

All of our samples were stabilized with taxol, which binds to and stabilizes the zinc-sheets against low temperature depolymerization, much as it does in microtubules. Tubulin bound to taxol can polymerize even in the absence of GTP. This suggests that the presence either of the γ phosphate or of taxol stabilizes the tubulin conformation that favors polymerization. The 3.7 Å map displays clear density for the taxol molecule that has been included in the atomic model using the crystal structure of taxotere, a taxol analogue. The position and orientation of the taxoid are consistent with a number of experimental observations. Crosslinking studies have localized residues β:1-31 near the C13 side chain of taxol (Rao et al. 1994), which in the model is close to the end of the helix H1 near β:25. The C2 phenyl group of taxol can be crosslinked to the region β:217–231 (Rao et al. 1995), and in the model is close to β:212–222. A recent study has identified the mutation of Phe272 to valine as related to taxol resistance in a cell culture line (Giannakakou et al. 1997). Phe272 sits in the beta strand on the back of the taxoid, and its side chain interacts with the C3′ phenyl ring of taxol. Interestingly, one of the significant differences between the α and β monomers is at the taxol site. An 8-residue insertion in α tubulin is situated in a loop that covers the region that corresponds to the taxol binding site in β tubulin.

The nature of other drug binding sites is of particular interest, and while no drugs besides taxol have been visualized in the sheets, some insights can be gained on the binding of other drugs by integrating biochemical data into the model structure. There is much data, for example, on the colchicine binding site. Crosslinking studies have shown the proximity of the binding site to Cys356 in β, with the sulfur of the cysteine expected to be within 3 Å of the C3 oxygen on the A ring of colchicine (Bai et al. 1996). Other experiments show crosslinking of colchicine to two other sites, one within residues 1–46 and one in 216–243, also in β (Uppuluri et al. 1993). Furthermore, the crosslinking of Cys241 and Cys356 in β tubulin abolishes binding of colchicine (Roach and Ludueña 1984). It has also been shown that colchicine interacts with α, although the primary contacts appear to be with β, and it has been suggested that the B ring should project toward α (Wolff and Knipling 1995; Banerjee et al. 1997). Thus the region of tubulin that interacts with colchicine, near the α-β inter-

face and on the side facing the microtubule lumen, is well enough characterized to model the interaction. In Fig. 5, a colchicine molecule in the conformation that was determined by x-ray crystallography has been modeled into the dimer structure to indicate the location that is suggested by the available evidence. Colchicine is known to bind in a two-step process, which is generally interpreted as comprising a rapid association followed by stronger binding associated with a conformational change in the tubulin dimer (Garland 1978; Díaz and Andreu 1991). It is tempting to suppose that the conformational change may involve an increase in the contact to residues in helix H2 of α, which is just above the colchicine in this model. This hypothetical model may suggest rational experiments aimed at further understanding the nature of colchicine binding as well as related effects. For example, it is not yet clear why colchicine enhances the intrinsic GTPase activity of tubulin or how this effect would vary among the different isotypes (Banerjee 1997). This type of question can be addressed more directly now on the basis of the structure.

Tubulin is the second self-assembling protein of the eukaryotic cytoskeleton whose structure has been solved. In the case of actin, the crystal structure was that of the unpolymerized protein (in fact, bound to a second molecule to prevent self-assembly) (Kabsch et al. 1990). Understanding the structure of the polymerized form involved the complex modeling of actin into the F-actin fibers (Holmes et al. 1990), with results not always unambiguously clear. On the other hand, the structure of tubulin has been obtained in a polymerized form. Although the interactions between protofilaments in the zinc-sheets and in microtubules have to be different, the extensive interactions between monomers and dimers at the longitudinal interfaces are certain to be extremely similar between these two polymer forms. Docking of the tubulin dimer into the microtubule thus involves only two degrees of freedom, a rotation with respect to the protofilament axis and a translation parallel to it (manuscript in preparation). Such a model of the microtubule will reveal the sites of lateral interactions in microtubules, completing our knowledge of the tubulin residues involved in microtubule polymerization.

Conclusion

The atomic model of tubulin allows us to begin to understand the biophysical properties of microtubules. We can identify residues involved in nucleotide binding and polymerization along the protofilament, and can model interactions between protofilaments and with drugs and other proteins. As we extend the resolution and refine the model to more accurately define the side chain orientations, the significance of particular side chain interactions in microtubule polymerization and stability should become more clear. We should also be able to understand how tubulin mutations produce their particular phenotypes. Some of these can already be understood. For example, removing charged residues in the motor-binding regions of β is lethal (Reijo et al. 1994), presumable due to an unfavorable interaction with the motors. We anticipate being able to relate differences among isotypes to their different properties. The function of various post-translational modifications may become clear, although at the moment some are quite mysterious. For example, Lys40 in α is frequently acetylated. Lys40 is in one of the loops that protrude into the lumen of the microtubule, and it is not yet clear what interactions would be modified by this acetylation. The model already provides the basis for understanding a number of observations about tubulin's behavior, and should suggest a new generation of experiments aimed at further understanding in detail the mysteries of this vital part of the cytoskeleton.

Acknowledgements This work has been supported by National Institutes of Health Grants GM46033 and GM51487 and by the Office of Health and Environmental Research, U.S. Department of Energy under Contract DE-AC03-76F00098.

References

Bai R, Pei X, Boye O, Getanunt Z, Grover S, Bekisz J, Nguyen N, Brossi A, Hamel E (1996) Identification of cysteine 354 of β-tubulin as part of the binding site for the A ring of colchicine. J Biol Chem 271:12639–12645

Banerjee A (1997) Differential effects of colchicine and its B-ring modified analog MTPT on the assembly-independent GTPase activity of purified β-tubulin isoforms from bovine brain. Biochem Biophys Res Commun 231:698–700

Banerjee S, Chakrabarti G, Bhattacharyya B (1997) Colchicine binding to tubulin monomers: a mechanistic study. Biochemistry 36:5600–5606

Caplow M, Ruhlen RL, Shanks J (1994) The free energy of hydrolysis of a microtubule-bound nucleotide triphosphate is near zero: all of the free energy for hydrolysis is stored in the microtubule lattice. J Cell Biol 127:779–788

Cross D, Dominguez J, Maccioni RB, Avila J (1991) MAP-1 and MAP-2 binding sites at the C-terminus of β-tubulin. Studies with synthetic tubulin peptides. Biochemistry 30:4362–4366

Díaz JF, Andreu JM (1991) Kinetics of dissociation of the tubulin-colchicine complex. J Biol Chem 266:2890–2896

Downing KH, Jontes J (1992) Projection map of tubulin in zinc-induced sheets at 4 Å resolution. J Struct Biol 109:152–159

Downing KH, Nogales E (1998) Tubulin and microtubule structure. Curr Opin Cell Biol 10:16–22

Fan J, Griffiths AD, Lockhart A, Cross RA, Amos LA (1996) Microtubule minus ends can be labelled with a phage display antibody specific to α-tubulin. J Mol Biol 259:325–330

Garland DL (1978) Kinetics and mechanism of colchicine binding to tubulin: evidence for ligand-induced conformational change. Biochemistry 17:4266–4272

Giannakakou P, Sackett DL, Kang Y-K, Zhan Z, Buters JTM, Fojo T, Poruchynsky MS (1997) Paclitaxel-resistant human ovarian cancer cells have mutant β-tubulins that exhibit impaired paclitaxel-driven polymerization. J Biol Chem 272:17118–17125

Hirose K, Fan J, Amos LA (1995) Re-examination of the polarity of microtubules and sheets decorated with kinesin motor domain. J Mol Biol 251:329–333

Holmes KC, Popp D, Gebhard W, Kabsch W (1990) Atomic model of the actin filament. Nature 347:44–49

Kabsch W, Mannherz HG, Suck D, Pai EF, Holmes KC (1990) Atomic structure of the actin: DNase I complex. Nature 347:37–44

Krauss E, Little M, Kempf T, Hofer-Warbinek R, Ade W, Ponstingl H (1981) Complete amino acid sequence of β-tubulin from porcine brain. Proc Natl Acad Sci USA 78:4156–4160

Larsson H, Wallin M, Edstrom A (1976) Induction of a sheets polymer of tubulin by Zn^{2+}. Exp Cell Res 100:104–110

Mandelkow E-M, Herrmann M, Rühl U (1985) Tubulin domains probed by limited proteolysis and subunit-specific antibodies. J Mol Biol 185:311–327

Mitchison TJ (1993) Localization of an exchangeable GTP binding site at the plus end of microtubules. Science 261:1044–1047

Nogales E, Wolf SG, Downing KH (1998a) Structure of the tubulin dimer by electron crystallography. Nature 391:199–203

Nogales E, Downing KH, Amos LA, Löwe J (1998b) Tubulin and FtsZ form a distinct family of GTPases. Nature Struct Biol 5:451–458

Nogales E, Wolf SG, Khan IA, Ludueña RF, Downing KH (1995) Structure of tubulin at 6.5 Å and location of the taxol-binding site. Nature 375:424–427

Rao S, Krauss NE, Heerding JM, Orr GA, Horwitz SB (1994) 3′-(p-Azidobenzamido)taxol photolabels the N-terminal 31 amino acids of β-tubulin. J Biol Chem 269:3132–3134

Rao S, Orr GA, Chaudhary AG, Kingston DGI, Horwitz SB (1995) Characterization of the taxol binding site on the microtubule: 2-(*m*-Azidobenzoyl)taxol photolabels a peptide (amino acids 217–231) of β-tubulin. J Biol Chem 270:20235–20238

Reijo RA, Cooper EM, Beagle GJ, Huffaker TC (1994) Systematic mutational analysis of the yeast β-tubulin gene. Mol Biol Cell 5:29–43

Roach MC, Ludueña RF (1984) Different effects of tubulin ligands on intrachain cross-linking of beta-tubulin. J Biol Chem 259: 12063–12071

Scheffzek K, Ahmadian M, Kabsch W, Wiesmuller L (1997) The Ras-RasGAP complex: structural basis for GTPase activation and its loss in oncogenic Ras mutants. Science 277:333–338

Uppuluri S, Knipling L, Sackett DL, Wolff J (1993) Localization of the colchicine-binding site of tubulin. Proc Natl Acad Sci USA 90:11598–11602

Wolf SG, Nogales E, Kikkawa M, Gratzinger D, Hirokawa N, Downing KH (1996) Interpreting a medium-resolution model of tubulin: comparison of zinc-sheet and microtubule structure. J Mol Biol 263:485–501

Wolff J, Knipling L (1995) Colchicine binding by the “isolated” β-monomer of tubulin. J Biol Chem 270:16809–16812